Applied Physics B (2018) 124:99
https://doi.org/10.1007/s00340-018-6961-6

Applied Physics B
Lasers and Optics

Generation of bound states of pulses in a SESAM mode-locked Cr:ZnSe laser

Xiangbao Bu[1] · Yuhang Shi[1] · Jia Xu[2] · Huijuan Li[1] · Pu Wang[1]

Received: 26 January 2018 / Accepted: 23 April 2018 / Published online: 9 May 2018

Abstract
We report on the generation of bound states of pulses in a SESAM mode-locked Cr:ZnSe laser around 2415 nm. A thulium-doped double-clad fiber laser at 1908 nm was used as the pump source. Bound states with various pulse separations at different dispersion regimes were obtained. Especially, in the anomalous dispersion regime, vibrating bound state of solitons exhibiting an evolving phase was obtained.

1 Introduction

In the last few years, we evidence a growing interest to Cr^{2+}-doped lasers of the II–VI family operating in the "molecular fingerprint" range between 2 and 3.5 μm which are rather efficient in comparison to multi-stage parametric frequency converters. These lasers are highly important for applications such as ultrafast spectroscopy, high-resolution and broadband spectroscopy, frequency metrology, synthesis of mid-IR optical frequency combs, nano- and micro-structuring in semiconductors (e.g., for fabrication of Si-photonic structures), trace-gas sensing, as well as for continuum generation in the mid-IR. Among these crystals, Cr:ZnS and Cr:ZnSe are nicely suitable for high-power femtosecond pulse generation due to their broad gain, good thermo-optical and thermo-mechanical properties. Conveniently, Cr:ZnS/Se lasers can be pumped by cost-effective, efficient, and reliable erbium (Er) and thulium (Tm) fiber lasers [1, 2]. The first femtosecond operation (80 fs) Cr:ZnSe laser using SESAM has been reported in 2006 [3]. Kerr-lens mode-locked (KLM) laser regime was achieved in 2009 using a single-crystal Cr:ZnSe sample [4]. There have also been a number of reports on femtosecond Cr:ZnS/Se lasers passively mode-locked by graphene. Pulse duration as short as 41 fs [5] was obtained with this technique. Kerr-lens mode-locking in polycrystalline Cr:ZnS and Cr:ZnSe was demonstrated in 2014 [6] and has led to significant improvements in the output parameters of ultrafast mid-IR oscillators in terms of both average power and pulse energy. Recent achievements include < 29 fs KLM Cr:ZnS oscillator [7], 43 fs Cr:ZnSe oscillator [8] and 47 fs Cr:ZnSe oscillator with high spectral purity in N_2 atmosphere [9]. Other achievements include 140 W continuous wave (CW) Cr:ZnSe MOPA system, 50 mJ Cr:ZnSe nanosecond MOPA system and Cr:ZnSe CPA system with a peak power of 5 GW [10–12]. Repetition rates as high as 1.2 GHz KLM Cr:ZnS laser were also obtained [13]. The KLM Cr:ZnS/Se lasers are free of the bandwidth limitation and allow increasing the pump power, but these come at the expense of self-starting difficulty.

In view of many applications, it is particularly important to control pulse emission characteristics. For some cavity configurations and relatively large pumping powers, single-pulse operation is not stable, and the laser switches to multiple-pulsing operation [14]. Multiple pulsing manifests either in largely separated pulses that may lead to harmonic mode-locking, or in bound states of close pulses. Stable bound states consist of pulse pairs or more pulses propagating with stable interpulse separation and relative phase. Multiple pulsing is not restricted to fiber lasers [15, 16], and has also been reported in the area of ultrashort bulk lasers. With a soft-aperture KLM Ti:sapphire laser, other than the harmonic mode-locking, multiple-pulse operations with π and $\pi/2$ phase differences were also observed in 2002 [17].

This article is part of the topical collection "Mid-infrared and THz Laser Sources and Applications" guest edited by Wei Ren, Paolo De Natale and Gerard Wysocki.

✉ Pu Wang
wangpuemail@bjut.edu.cn

[1] Institute of Laser Engineering, Beijing Engineering Research Center of Laser Applied Technology, Beijing University of Technology, Beijing 100124, China

[2] Max-Planck-Institute of Quantum Optics, Hans-Kopfermann-Str. 1, 85748 Garching, Germany

Bound states of solitons with rotating phase difference and separated by 917.5 fs were observed with a diode-pumped Yb:KGW mode-locked laser in 2004 [18]. The influences of intra-cavity dispersions on the multipulse operation of a KLM Ti:sapphire laser were studied in 2008 [19]. Soliton bound states were obtained in an 85.7 MHz repetition rate mode-locked semiconductor disk laser in 2013 [20]. Except for the double-pulsed mode-locking with a reproducible pulse separation of about 2.4 ps in a KLM polycrystalline Cr:ZnS laser [21], there has been no report on the investigation of bound states in Cr^{2+}-doped II–VI lasers.

Here, we report a SESAM mode-locked Cr:ZnSe laser pumped by a Tm-doped double-clad fiber laser at 1908 nm. Stable bound states with various pulse separations at different dispersion regimes were obtained.

2 Experimental setup

Figure 1 shows a schematic of the SESAM mode-locked Cr:ZnSe laser. The gain medium was pumped by a home-made 1908-nm Tm-doped fiber laser. The laser was based on a double-clad Tm-doped fiber with 25 μm, 0.09-NA circular core and 400-μm, 0.46-NA, octagonal inner cladding, and its absorption coefficient at 793 nm was 2.4 dB/m. The active fiber was 3.2 m long wrapped around a 20-cm-diameter mandrel. The fiber was cooled at a constant temperature of 13 °C to provide thermal management and improve laser efficiency, because the performance of Tm ions highly depended on temperature as a quasi three-level system. A pair of fiber Bragg gratings (FBGs) at a wavelength of 1908 nm (one had high reflection $R = 99\%$, and the other had partial reflection $R = 10.9\%$) was separately spliced to each end of the Tm-doped fiber to complete a laser cavity. The Tm-doped fiber and all the other optical components were fusion spliced, providing an all-fiber configuration for the whole 1908-nm fiber laser system. The collimator was also an isolator which can prevent the feedback light. The light from the diode-pumped Tm-doped fiber laser was converted to linearly polarized light through a Glan-Laser polarizer and the output power was optimized by a quarter wave plate.

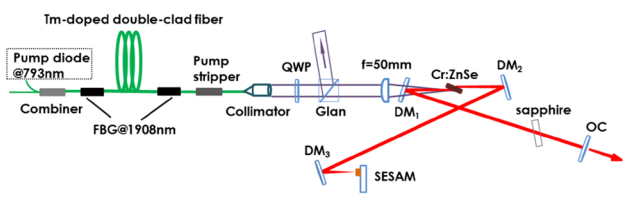

Fig. 1 Schematic of the SESAM mode-locked Cr:ZnSe laser pumped by 1908-nm fiber laser. *FBG* fiber Bragg grating, *QWP* quarter wave plate, *DM* dichroic concave mirror, *OC* output coupler

The pump beam from the fiber laser was focused on the Cr:ZnSe crystal by a lens with 50 mm focal length. The 5-mm-thick single-crystal Cr:ZnSe providing 75% of pump absorption was wrapped with an indium foil and mounted tightly in a water-cooled copper heat sink maintained at 13 °C. The crystal was positioned at Brewster angle in the middle of the astigmatism compensated x-type cavity. This cavity consisted of two concave mirrors with 75 mm radius of curvature (r.o.c.), a folding 75-mm r.o.c. mirror, which focused light on a commercial SESAM with a radius of about 32 μm and a plane-parallel output coupler (OC). The SESAM has been designed to provide modulation depth of 0.6%, relaxation time of 10 ps, and saturation fluence of 90 μJ/cm^2. The designed central wavelength of the SESAM was 2400 nm and its reflectivity band covered the range between 2300 and 2650 nm. The output coupler with transmission of 4.5% in the range of 2350–2550 nm was used for coupling-out. The total length of the cavity was about 1.18 m, corresponding to a repetition rate close to 126.4 MHz. All measurements were performed in the open air with 20 °C room temperature and relative humidity 35–48%. The spectrum was analyzed by a commercial FTIR spectrometer (OSA 205, Thorlabs). The pulse duration was measured by a home-made collinear autocorrelator using two-photon absorption in an InGaAs photodiode.

3 Results and discussion

The CW operation was characterized with a flat high reflector in the SESAM arm. The pump threshold and maximum output power were measured to be 400 and 900 mW at the pump power of 6.8 W, respectively, with slope efficiency 14.3%. In this case, the laser was operated in the middle of the lower stability region (corresponding to shorter mirror spacing between DM_1 and DM_2). With a SESAM and a concave mirror in place, the threshold pump power increased to 920 mW as the SESAM provided high losses in the cavity and thus redefined the threshold. During the optimization process, the mirror spacing between DM_1 and DM_2 was kept to be constant.

Different experimental scenarios leading to the generation of bound states of pulses have been reported. In some cases, bound states of pulses can be generated abruptly from CW operation, increasing only the pump power. For other configurations, the laser switches from CW to single-pulse regime and then to three- or two-bound-state regime when the pump power is increased [14]. Let us now present one of the scenarios. The SESAM soldered on a copper heat sink was handled by a mirror mount. The mirror mount was placed on a precision translation stage which has a travel range of 13 mm and a sensitivity of < 1 μm. At first, the position of the SESAM was optimized by tuning the translation

stage to maximize the output power. The maximum power position was located around the focus of DM_3. Second, the precision translation stage was carefully tuned in the direction away from DM_3 and the output power decreased gradually. According to the ABCD matrix propagation theory, the lasing mode spot size on the SESAM also decreased. When the pump power exceeded 4.2 W, unstable pulse trains could be observed within a certain region of several tens of micrometers. Then by gradually tilting the angle of the SESAM in horizontal direction, mode-locking operation of multipulse was reached. It was confirmed by the fact that we obtained an abrupt transition from an irregular spectrum to a regularly modulated spectrum. As the pump power was carefully increased to 4.6 W, a stable tightly bound state of pulse pair was obtained by further adjustments on the angle of the SESAM. Radio frequency (RF) spectrum of the bound state was measured with a RF spectrum analyzer (Agilent N9030A) and an infrared HgCdTe optoelectronic detector with a rise time of <2 ns (VIGO System model PCI-9). As revealed in Fig. 2, the fundamental beat note is 126.42 MHz with a high extinction down to 58 dB, confirming the mode-locking stability. The RF spectrum in the inset, with a resolution bandwidth (RBW) of 100 kHz, shows regular peaks at multiples of the cavity fundamental frequency over an 800 MHz span. The pedestal in the inset is caused by the RF spectrum analyzer. The maximum average output power of the two-pulse bound state was 342 mW under the pump power of 4.8 W. Figure 3a shows the optical spectrum of the bound state. It is strongly modulated, which is a direct consequence of a precise phase relationship maintained between the closely spaced two pulses. The period of the spectral modulation is 12.2 nm, and according to the Fourier transformation it corresponds to a soliton separation of about 1.6 ps in the time domain. Figure 3b shows the autocorrelation trace of the bound state. As the two lateral peaks in Fig. 3b corresponding to the overlap in time of consecutive pulses show clear interference structures, we can conclude that the phases of the two pulses were locked. The asymmetric structure of the spectrum with unequal central maxima indicates that the phase difference of the tightly bound state is closer to $-\pi/2$ [22]. The autocorrelation trace also shows that the pulse separation is about 1.6 ps, which is in agreement with the spectral modulation period of 12.2 nm. Considering that the central peak of the autocorrelation trace has a pulse width of about 800 fs, the pulse separation is two times of the pulse width.

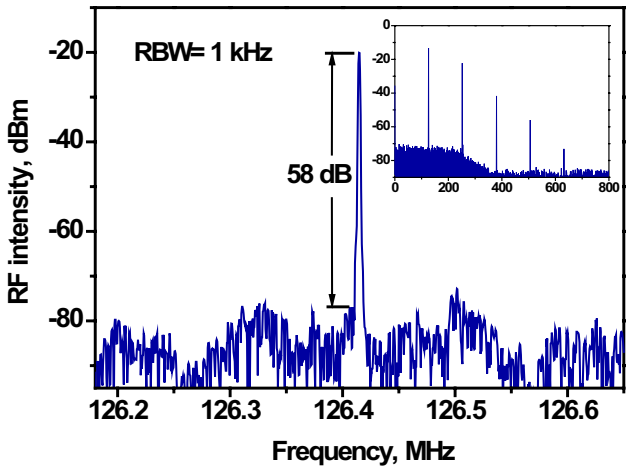

Fig. 2 RF spectrum of a stationary bound state over a 470 kHz span (inset: RF spectrum over an 800 MHz span)

Inserting a 5-mm-thick sapphire plate into the cavity brought the net group delay dispersion (GDD) to -410 fs^2 and resulted in anomalous (soliton) dispersion regime. For low pump power, CW operation was observed. When the pump power reached 4.3 W, the mode-locking threshold was reached by fine-tuning the position and angle of the SESAM and the laser delivered a three-pulse bound state. The maximum average output power of the bound state was increased to 403 mW with respect to incident pump power of 4.7 W. We attribute the increase of average power to the cavity mode optimization by the sapphire plate. Further increasing the pump power resulted in more deterioration of the beam quality and loss of mode-locking stability. Figure 4a shows the optical spectrum of a bound state of solitons, which is regularly modulated with high contrast of the modulation

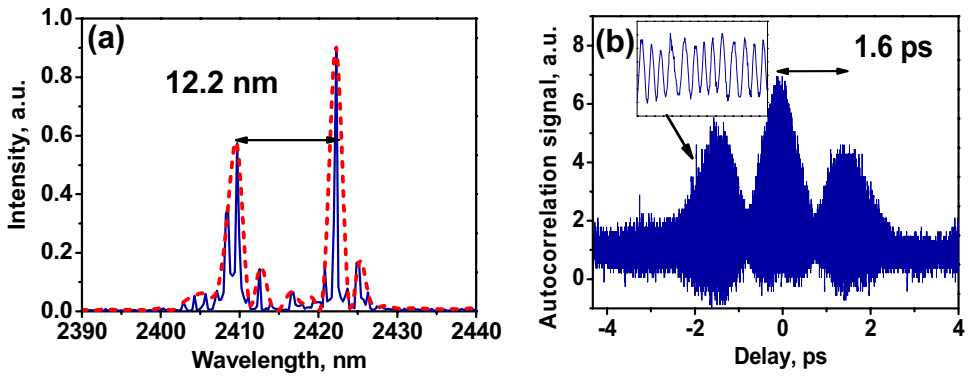

Fig. 3 Experimental observation of a stationary bound state of pulse pair without dispersion compensation: **a** the optical spectrum; **b** the autocorrelation trace

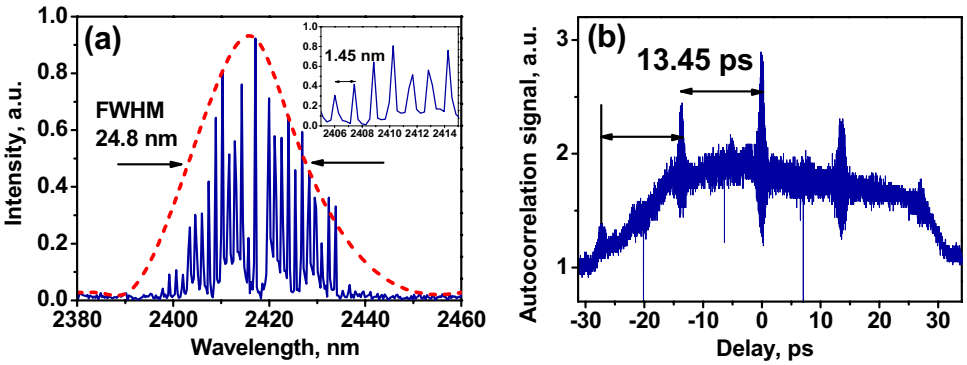

Fig. 4 **a** The optical spectrum of a three-pulse bound state in anomalous dispersion regime (inset: magnified view of the channeled spectrum); **b** the autocorrelation trace of the three-pulse bound state

depth. The spectrum is centered at 2415 nm with a full width at half maximum (FWHM) of 24.8 nm. A zoom of this spectrum is presented in the inset of Fig. 4a. The period of the spectral modulation is 1.45 nm, and according to the Fourier transformation it corresponds to a soliton separation of about 13.45 ps in the time domain. The autocorrelation trace (Fig. 4b) also shows that the pulse separation is about 13.45 ps, which is in agreement with the spectral modulation period of 1.45 nm. The measured FWHM of the central peak is about 1.15 ps, corresponding to 608 fs pulse duration if a sech^2 profile is assumed. The pulse separation is 22 times of the pulse width. Notice the presence of interference fringes in the lateral peaks of the autocorrelation trace in Fig. 4b, indicating that the three pulses were phase locked. However, the precise phase relationship between the three pulses was difficult to measure because of the large pulse separation. With large soliton separation the direct soliton–soliton interaction becomes weak. The phase difference between the bound state of solitons is no longer fixed at the π or $\pi/2$, but varies from case to case [23]. Moreover, especially the unmodulated part of the spectrum allows us to conclude that we observed a bound state with an evolving phase [24]. These experimental features are the result of the time averaging effect of a vibrating bound state of solitons, as originally shown in [25].

As we have shown in Fig. 5, as the laser operation conditions were slightly shifted, three bound state spectra with different contrast of modulation depth were obtained. In Fig. 5a–c, we clearly observe an evident loss of contrast over the spectral fringes from near 100–90%. As shown in Fig. 5d, the three different spectra have the same modulation period of 1.45 nm indicating a fixed pulse separation during

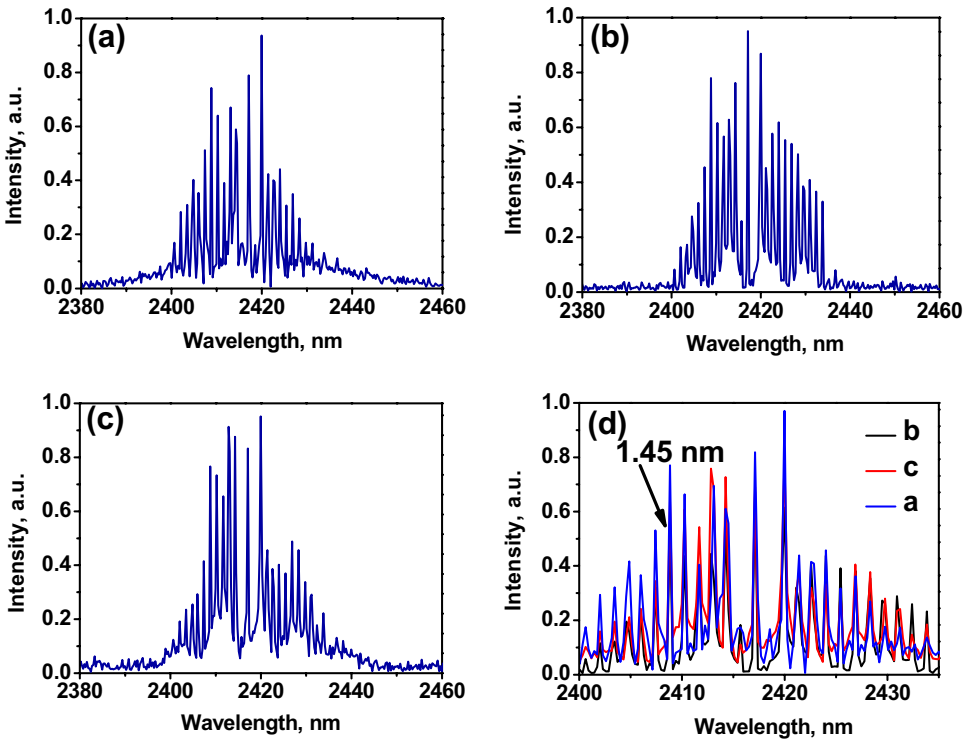

Fig. 5 Influence of the averaging process on the measured spectral profile: **a**–**c** different contrast of modulation depth; **d** the phases of different bound states are oscillating with amplitudes and the pulse separations are fixed

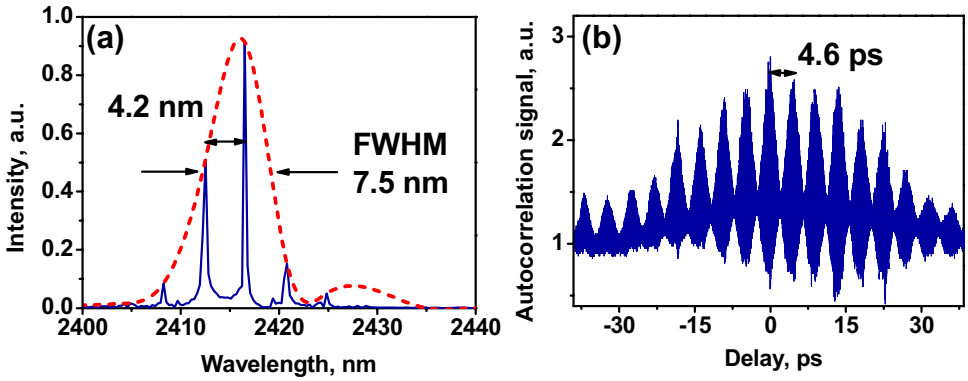

Fig. 6 Experimental observation of a bound state of multiple pulses in chirped-pulse dispersion regime: **a** the optical spectrum; **b** the autocorrelation trace

the phase evolving. For an oscillating phase difference and a fixed separation, the average effect led to a decrease in the modulation depth in dependence on the phase variation of the amplitude. In the anomalous dispersion regime, bound states of solitons with other pulse separation were not obtained.

Replacing the 5-mm-thick sapphire plate with a 3-mm one in the cavity brought the net GDD to 699 fs^2 and resulted in normal (chirped-pulse) dispersion regime. Though normal-dispersion mode-locked lasers generally work on a single-pulse regime due to the large chirp of the pulses, we also directly obtained bound state of multiple pulses from CW operation in the laser. The maximum average output power of the bound state was 370 mW with respect to incident pump power of 4.7 W. The optical spectrum is shown in Fig. 6a centered at 2416 nm with a FWHM of 7.5 nm. The period of the spectral modulation is 4.2 nm, and according to the Fourier transformation it corresponds to a soliton separation of about 4.6 ps in the time domain. Indeed, the spectrum exhibits a modulation of nearly 100% contrast and has the features that the phase difference of the bound states has a fixed value of $-\pi/2$. The autocorrelation trace in Fig. 6b also shows that the pulse separation is 4.6 ps, which is in agreement with the spectral modulation period of 4.2 nm. Considering that the central peak of the autocorrelation trace has a pulse width of about 1.58 ps, the pulse separation is 3 times of the pulse width. The peak-to-peak soliton separation is smaller than 5 times of the pulse width. They belong to the category of so-called tightly bound states of pulses. In our experiments, once the bound state of multiple pulses was obtained, a tiny change in the pump power did not vary the pulse separation and their phase difference of $-\pi/2$. The experimental features indicate that the bound state of pulses is an intrinsic feature of mode-locked solid-state lasers and is independent of pulse profiles.

Obviously, the mode-locking mechanism strongly influences the generation of bound states. In this paper, the generation mechanism can be attributed to the oversaturation of the SESAM and the excessive nonlinear phase shift that cannot be compensated by dispersion [26]. Under high pump power, the small beam radius on the SESAM results in an energy fluence many times the saturation fluence. Therefore, the strongly saturated SESAM provides reduced discrimination between single pulse and multipulse [27]. The excessive nonlinear phase shift can be attributed to two reasons. First, the tightly focused cavity mode in the Cr:ZnSe crystal results in a high peak power density under high pump power. Second, the third-order nonlinearity n_2 of Cr:ZnSe is 170×10^{-20} m^2/W, which is about 56 times larger than that of sapphire [28].

4 Conclusion

In conclusion, we report the generation of bound states of pulses in a SESAM mode-locked Cr:ZnSe laser pumped by a thulium-doped double-clad fiber laser at 1908 nm. Without dispersion compensation, stable pulse pair with a separation of 1.6 ps was observed. In anomalous dispersion regime, vibrating bound state of three solitons was obtained. This state of bound solitons had an independently evolving phase, which resulted in an incomplete modulation of the optical spectrum. In chirped-pulse regime, bound state of multiple pulses with 4.6 ps separation was obtained. Bound states of pulses seem to be the most stable states in our passively mode-locked Cr:ZnSe laser.

Acknowledgements The authors acknowledge funding support from the Natural National Science Foundation of China (61527822, 61235010).

References

1. S. Mirov, V. Fedorov, D. Martyshkin, I. Moskalev, M. Mirov, S. Vasilyev, Progress in Mid-IR lasers based on Cr and Fe-Doped II–VI chalcogenides. IEEE J. Sel. Top. Quantum Electron. **21**(1), 292–310 (2015)
2. I.T. Sorokina, E. Sorokin, Femtosecond Cr^{2+}-based lasers. IEEE J. Sel. Top. Quantum Electron. **21**(1), 273–291 (2015)
3. I.T. Sorokina, E. Sorokin, T. Carrig, Femtosecond pulse generation from a SESAM mode-locked Cr:ZnSe laser. Conference on

Lasers and Electro-Optics, (Optical Society of America, 2006), paper CMQ2
4. M.N. Cizmeciyan, H. Cankaya, A. Kurt, A. Sennaroglu, Kerr-lens mode-locked femtosecond Cr^{2+}: ZnSe laser at 2420 nm. Opt. Lett. **34**(20), 3056–3058 (2009)
5. N. Tolstik, E. Sorokin, I.T. Sorokina, Graphene mode-locked Cr:ZnS laser with 41 fs pulse duration. Opt. Express **22**(5), 5564–5571 (2014)
6. S. Vasilyev, M. Mirov, V. Gapontsev, Kerr-lens mode-locked femtosecond polycrystalline Cr^{2+}:ZnS and Cr^{2+}:ZnSe lasers. Opt. express **22**(5), 5118–5123 (2014)
7. S. Vasilyev, I. Moskalev, M. Mirov, S. Mirov, V. Gapontsev, Three optical cycle mid-IR Kerr-lens mode-locked polycrystalline Cr^{2+}:ZnS laser. Opt. Lett. **40**(21), 5054–5057 (2015)
8. S. Vasilyev, M. Mirov, V. Gapontsev, High power Kerr-Lens mode-locked femtosecond mid-ir laser with efficient second harmonic generation in polycrystalline Cr^{2+}:ZnS and Cr^{2+}:ZnSe. Advanced Solid State Lasers, (Optical Society of America 2014), paper. AM3A. 3
9. Y. Wang, T.T. Fernandez, N. Coluccelli, A. Gambetta, P. Laporta, G. Galzerano, 47-fs Kerr-lens mode-locked Cr:ZnSe laser with high spectral purity. Opt. Express **25**(21), 25193–25200 (2017)
10. I. Moskalev, S. Mirov, M. Mirov, S. Vasilyev, V. Smolski, A. Zakrevskiy, V. Gapontsev, 140 W Cr:ZnSe laser system. Opt. express **24**(18), 21090–21104 (2016)
11. M. Yumoto, N. Saito, S. Wada, 50 mJ/pulse, electronically tuned Cr:ZnSe master oscillator power amplifier. Opt. Express **25**(26), 32948–32956 (2017)
12. E. Slobodchikov, L.R. Chieffo, K.F. Wall, High peak power ultrafast Cr:ZnSe oscillator and power amplifier. Solid state lasers XXV: technology and devices. Int Soc Opt Photon **9726**: 972603 (2016)
13. S. Vasilyev, I. Moskalev, M. Mirov, V. Smolski, S. Mirov, V. Gapontsev, *Kerr-lens mode-locked middle IR polycrystalline Cr:ZnS laser with a repetition rate 1.2 GHz*. Advanced Solid State Lasers, (Optical Society of America 2016), paper, AW1A. 2
14. B. Ortaç, A. Hideur, T. Chartier, M. Brunel, P. Grelu, H. Leblond, F. Sanchez, Generation of bound states of three ultrashort pulses with a passively mode-locked high-power Yb-doped double-clad fiber laser. IEEE Photon. Technol. Lett. **16**(5), 1274–1276 (2004)
15. P. Wang, C. Bao, B. Fu, X. Xiao, P. Grelu, C. Yang, Generation of wavelength-tunable soliton molecules in a 2-μm ultrafast all-fiber laser based on nonlinear polarization evolution. Opt. Lett. **41**(10), 2254–2257 (2016)
16. L. Li, Q. Ruan, R. Yang, L. Zhao, Z. Luo, Bidirectional operation of 100 fs bound solitons in an ultra-compact mode-locked fiber laser. Opt. express **24**(18), 21020–21026 (2016)
17. J.H. Lin, W.F. Hsieh, H.H. Wu, Harmonic mode locking and multiple pulsing in a soft-aperture Kerr-lens mode-locked Ti: sapphire laser. Opt. Commun. **212**(1), 149–158 (2002)
18. G. Paunescu, J. Hein, R. Sauerbrey, 100-fs diode-pumped Yb: KGW mode-locked laser. Appl. Phys. B **79**(5), 555–558 (2004)
19. J. Wu, H. Cai, X. Han, H. Zeng, Multi-pulse operation of a Kerr-lens mode-locked femtosecond laser. Chin. Opt. Lett. **6**(1), 76–78 (2008)
20. M. Butkus, E.A. Viktorov, T. Erneux, C.J. Hamilton, G. Maker, G.P.A. Malcolm, E.U. Rafailov, 85.7 MHz repetition rate mode-locked semiconductor disk laser: fundamental and soliton bound states. Opt. express **21**(21), 25526–25531 (2013)
21. N. Tolstik, E. Sorokin, I.T. Sorokina, Kerr-lens mode-locked Cr: ZnS laser. Opt. Lett. **38**(3), 299–301 (2013)
22. P. Grelu, F. Belhache, F. Gutty, J.M. Soto-Crespo, Phase-locked soliton pairs in a stretched-pulse fiber laser. Opt. Lett. **27**(11), 966–968 (2002)
23. X. Wu, D.Y. Tang, X.N. Luan, Q. Zhang, Bound states of solitons in a fiber laser mode locked with carbon nanotube saturable absorber. Opt. Commun. **284**(14), 3615–3618 (2011)
24. B. Ortaç, A. Zaviyalov, C.K. Nielsen, O. Egorov, R. Iliew, J. Limpert, F. Lederer, A. Tünnermann, Observation of soliton molecules with independently evolving phase in a mode-locked fiber laser. Opt. Lett. **35**(10), 1578–1580 (2010)
25. M. Grapinet, P. Grelu, Vibrating soliton pairs in a mode-locked laser cavity. Opt. Lett. **31**(14), 2115–2117 (2006)
26. J.M. Soto-Crespo, P. Grelu, Temporal multi-soliton complexes generated by passively mode-locked lasers. *Dissipative Solitons, Springer*. (2005). pp. 207–239
27. J.A. Der Au, D. Kopf, F. Morier-Genoud, M. Moser, U. Keller, 60-fs pulses from a diode-pumped Nd: glass laser. Opt. Lett. **22**(5), 307–309 (1997)
28. I.T. Sorokina, Cr^{2+}-doped II–VI materials for lasers and nonlinear optics. Opt. Mater. **26**(4), 395–412 (2004)